IJISET - International Journal of Innovative Science, Engineering & Technology, Vol. 1 Issue 10, December 2014.
www.ijiset.com
ISSN 2348 – 7968

Optical and Nonlinear Optical Properties, Thermal Analysis, Cyclic Voltammetry and DFT Studies: Green Synthesis Approach of Boronates Derived from Schiff Bases.

Rodrigo Chan-Navarro[1], Blanca M. Muñoz-Flores[1]*, Víctor M. Jiménez-Pérez[1], Ivana Moggio[2], Eduardo Arias [2], Gabriel Ramos-Ortíz[3], María C. García-López [1], Víctor Rosas-García[1], Perla Elizondo,[1]Mario Rodríguez.[3]

[1]Universidad Autónoma de Nuevo León, Facultad de Ciencias Químicas, Ciudad Universitaria, Av. Universidad s/n. C. P. 66451, Nuevo León, México.

[2]Centro de Investigación en Química Aplicada, Boulevard Enrique Reyna 140, 25294 Saltillo, México.

[3]Centro de Investigaciones en Óptica, A. P. 1-948, 37000, León Gto., México

Abstract

The boron atom deviation from salicylidenimino-plane might affect the nonlinear optical (NLO) response. We found that the formation of the N→B coordinative bond increases the optical nonlinear response in comparison with the free-ligand. The electronic properties for these compounds were investigated by cyclic voltammetry, UV-vis, and fluorescence spectroscopy. DFT theory at B3LYP/6-31G (d) level indicates the phenyl of boron is not involved in the electronic distribution and these orbital frontiers are extended along the electron donor (-NEt_2, -OMe) and acceptor (-NO_2) groups of each system. Also, we reported two different one-pot microwave-assisted syntheses of four organoboron compounds with and without solvent where the reaction yield and time are improved.

Key words: NLO, organoboron, Schiff bases, microwave, solventless reaction.

1. Introduction

In recent years, there has been considerable interest in the synthesis of boron compounds indifferent fields such as supramolecularchemistry[1];medicinal chemistry as anticancer agents in boron neutron capture therapy [2], materials chemistry as fluorescents probes [3], imaging materials [4], laser dyes [5], organic light-emitting diodes [6], organic field-effect transistors [7], photo-responsive materials [8], and nonlinear optics [9]. A great number of complexes have been prepared by condensation reaction between boronic acids and chelate ligands. However, it is important to mention that these complexes have been obtained in good yields using long reaction times (24-48 h) [10], even it has sometimes necessary to use organic acids as a catalyst [11]. Recently, syntheses of new boron compounds were prepared under microwave irradiation [12] and multicomponent reaction [13] with short reaction times and excellent yields has been reported. However, the synthesis under microwaves irradiation using many solid supports [14] is a very attractive and clean route for the preparation of organoboron compounds which so far has not been explored.

Nowadays, there is increased interest in developing new organic materials with large second and third order optical nonlinear (NLO) responses for application in photonic such as optical communication, all-optical switching, data processing, and optical limiting [15]. Our research group has studied second and third order nonlinear properties of push-pull boron compounds [16]. These results have showed that appropriate combination between electron withdrawing (A) and donating (D) groups and the formation of the coordinative bond N→B optimize the nonlinear effects. In particular, the use of bipolar systems to allow the modulation of HOMO-LUMO levels of conjugated molecules, which are directly related to the polarizabilitydegree [17]. In our ongoing studies on structural-optical response of boron compounds derived from Schiff bases, we present an environment-friendly one-pot synthesis method of boron compounds under microwave irradiation. A comparative study of linear and nonlinear optical properties, Raman spectroscopy, electrochemical and thermal properties as well as theoretical study between free-ligands and boron compounds are also reported.

ISSN 2348 – 7968

2. Experimental methods

2.1 Material and equipment

2-hidroxysalicylaldehydes, benzoylhydrazides, phenyl boronic acid, and solvents were obtained from Aldrich Chemical Company without further purification. Synthesis of boron compounds **1**-**4** derivatives of the Schiff bases have been already published [23]. Boron compounds were characterized by UV-vis spectroscopy and their physical properties. UV spectra were obtained with a Varian Cary-100 UV/VIS spectrophotometer and emission measurements were performed on a Perkin Elmer LS-55 luminescence spectrometer. The preparation of boron compounds **1**-**4** was performed on a microwave reactor Anton PaarMonowave 300®with a power of 40 W and 20 bars, specially designed for small scale microwave synthesis. Simultaneous thermal analyses (TGA-DTA) were carried out in the temperature range 25 to 600 °C under nitrogen atmosphere at a heating rate of 10 °C min^{-1} using a TA instruments-SDT 2960 thermal analyzer.

2.2Synthesis of boron compounds 1-4 under microwave irradiation with solvent

A solution of salicylaldehyde 0.050 g (0.260 mmol), benzoylhydrazide 0.035 (0.260 mmol) and phenylboronic acid 0.320 g (0.260 mmol) in acetonitrile (5 mL) was irradiated at 200 ^{o}C for 5 min. The progress of the reaction was monitored by thin layer chromatography every 60 seconds. After cooling to room temperature, the excess solvent was removed and solid precipitate was filtered and washed with hexane. Compound **1**: deep yellow solid (95%); m. p.: 153 ^{o}C. UV/Vis (THF): $\lambda_{abs/max}$, $\varepsilon_{max}*10^4$: 427 nm, 1.24 $M^{-1}cm^{-1}$; Compound **2**: light green solid (96%); m. p.: 151 ^{o}C. UV/Vis (THF): $\lambda_{abs/max}$, $\varepsilon_{max}*10^4$: 393 nm, 1.68 $M^{-1}cm^{-1}$; Compound **3**: light orange solid (94%); m. p.: 278 ^{o}C. UV/Vis (THF): $\lambda_{abs/max}$, $\varepsilon_{max}*10^4$: 458 nm, 0.96 $M^{-1}cm^{-1}$; Compound **4**: bright yellow solid (97%); m. p.: 242 ^{o}C. UV/Vis (THF): $\lambda_{abs/max}$, $\varepsilon_{max}*10^4$: 412 nm, 1.97 $M^{-1}cm^{-1}$.

2.3 Synthesis of boron compounds 1-4 under microwave irradiation solventless

A homogeneous mixture of salicylaldehyde 0.050 g (0.26 mmol), benzoylhydrazide 0.035 (0.26 mmol), phenylboronic acid 0.320 g (0.26 mmol), and 0.200 g (1.96 mmol) alumina free-solvent was irradiated at 200 ^{o}C for 5 min. The alumina was activated at 210^{o}C for 3 min before it was used, and then the reaction was carried out according to describe above. Compound **1**: deep yellow solid (71%); m.p.: 153 ^{o}C. UV/Vis (THF): $\lambda_{abs/max}$, $\varepsilon_{max}*10^4$: 427 nm, 3.16 $M^{-1}cm^{-1}$; Compound **2**: light green solid (83%); m. p.: 151 ^{o}C. UV/Vis (THF): $\lambda_{abs/max}$, $\varepsilon_{max}*10^4$: 393 nm, 2.20 $M^{-1}cm^{-1}$; Compound **3**: light orange solid (80%); m. p.: 278 ^{o}C. UV/Vis (THF): $\lambda_{abs/max}$, $\varepsilon_{max}*10^4$: 456 nm, 2.78 $M^{-1}cm^{-1}$; Compound **4**: bright yellow solid (88%); m. p.: 242 ^{o}C. UV/Vis (THF): $\lambda_{abs/max}$, $\varepsilon_{max}*10^4$: 414 nm, 2.20 $M^{-1}cm^{-1}$.

2.4 Third-harmonic generation experiment

The organic materials were studied in solid films using the guest (molecule)-host (polymer) approach. Ratios 70:30 wt.% of polystyrene (PS) and compounds under test were dissolved in tetrahydrofurane. The solid films were deposited on glass substrates of a 1 mm of thick by using the spin coating technique. The solid films had typical thickness between 400 and 480 nm with good optical quality. UV-Vis spectroscopy of spin-coated films was performed on a spectrophotometer Perkin-Elmer Lambda 900 (Fig. S18). The film thickness was measured by a NanosurfEasyscan 2 AFM at a scanning of 50 μm/s and an applied dynamic force of 2 mg. Third-order nonlinear susceptibility in solid film $\chi^{(3)}$ (-3ω, ω, ω, ω) were determinate according to the procedure reported in literature [18] by the Maker-fringes technique at the IR wavelength of 1300 nm. It consisted of Nd-YAG laser- pumped optical parametric oscillator (OPO) that delivered pulses of 7 ns at a repetition rate of 10 Hz. The idler beam of the OPO system tuned at 1300 nm was focused into the polystyrene films doped with the molecule of interest. Typical pump irradiance at sample position was about 0.5 $GWcm^{-2}$. The third harmonic beam emerging from films was separated from the pump beam by using a color filter and detected with a PMT and a lock-in amplifier. The third harmonic generation (THG) measurements were performed for incidents angles in the range from -40° to 40° with steps of 0.27°. Whole of the experiment was computer controlled. The Marker Fringer technique compares the third harmonic peak intensity $I^{3\omega}$from the substrate-film with that produced from the glass substrate alone. The nonlinear susceptibility $\chi^{(3)}$in a film of thickness $L_f$isdeterminate from equation (**1**):

ISSN 2348 – 7968

$$x^{(3)} = x_s^{(3)} \frac{2}{\pi}\left(\frac{L_{c,s}}{L_f}\right)\left(\frac{I_f^{3\omega}}{I_s^{3\omega}}\right)^{1/2} \quad \text{Eq. (1)}$$

Where $\chi_s^{(3)}$ and $L_{c,s}$ are the nonlinear susceptibility and coherence length, respectively, for the glass substrate at the fundamental wavelength. In our calculation, we consider $\chi_s^{(3)}$= 3.1 x 10^{-14}esu and $L_{c,s}$= 14 μm for the glass substrate. In any case, our samples satisfied the condition $L_f << L_{c,s}$ in which Eq. 1 is valid.

2.5 Raman Spectroscopy

Raman spectra were recorded on Horiba Xplora equipment, focusing the sample as powders on microscopic slide with a 10X objective. The excitation wavelength was 785 nm and the Nanoled power was 25% of total laser power (25 mW). Spectra were acquired with 10s acquisition time and 5 cycles, spectral resolution of 2 cm

2.6 Electrochemical analysis

The electrochemical properties of ligands and complexes (0.5 mmol) were investigated by cyclic voltammetry in a C3 Stand cell from Basi coupled to a ACM Gill AC potentiostat/galvanostat. All the experiments were performed at room temperature in CH_2Cl_2 and acetonitrile containing Bu_4NPF6 (0.1M) as the supporting electrolyte, platinum as a working electrode, Pt wire electrode as the counter electrode, Ag/AgCl electrode as the reference electrode and ferrocene/ferrocenium (FOC) as internal reference (*E*ox= 0.58 V, *E*red= 0.701 V); value of -4.8 eV below the vacuum level. The experiments were carried out under nitrogen atmosphere at a scanning rate of 50 mV/s in a complete cycle between -3.0 and +3.0 V or in separated windows. The molecular orbital energies HOMO and LUMO were calculated from the first oxidation (*E*ox) and reduction (*E*red) potentials with the relationship: *E* HOMO[LUMO]=[-exp(Emax (Ox[red] vs Ag/AgCl)]-4.8.

2.7 Theoretical calculations

All calculations were performed with Spartan v10 (Wavefunction. Inc). First the equilibrium conformer at ground state was found at AM1 level and then this geometry was further optimized through Density Functional Theory (DFT) calculations at the restricted B3LYP level with 6-31G(d) basis set. In the case of the theoretical absorption spectra, all calculations were done with GAMESS-US version 1 MAY 2013 (R1)[19]. All the structures were optimized at the B3LYP [20]/6-31G* level of theory, both in the gas phase and with the PCM solvent model. The solvents specified by the PCM solvent model [21] were acetone (EPS=20.70 D), tetrahydrofurane (EPS=7.58 D), chloroform (EPS=4.90 D) and toluene (EPS=2.38 D). The optimized structures were subjected to vibrational analysis to ensure they were stationary points on the energy hypersurface, yielding only real vibrational frequencies. The excitation energies were calculated using TDDFT single points at the B3LYP/6-311++G** level on the previously optimized geometries, both in the gas phase and with PCM solvent model. The three lowest roots were calculated in all cases. Convolution of the resulting excited energies to simulated UV-Vis spectra was done with Gabedit v. 2.4.8. [22].

3. Results and Discussion

3.1 Synthesis

The boron complexes **1**-**4** were prepared under microwave irradiation as indicate in **Fig. 1**. The time and yield of reaction in acetonitrile and alumina as support are compared with conventional method in **Table 1**. In general, boron compounds were obtained in quantitative yields from 71 to 97%, where the best results corresponding the condensation reactions using acetonitrile as medium of reaction. However, the preparation of these complexes using alumina offers an excellent alternative with yields in a range from 71 to 88 % and a time of 5 minutes. The most significant change for both methods were given in reaction time, where it decreased about of 576 times less than conventional method previously reported [23]. Our best knowledge this is the first report on synthesis of boron complexes using an inorganic solid support under microwave irradiation.

ISSN 2348 – 7968

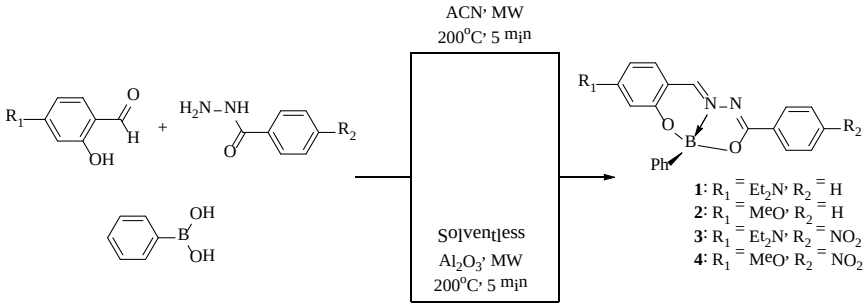

Fig. 1 Synthesis under microwave irradiation with solvent and solventless of boron compounds 1-4.

Table 1: Comparison of the time reaction and yields from different methods of compounds 1-4

Compound	Yield [%]			Reaction time [h]	[min]		Improved Time
	Conventional	Microwave		Conventional	Microwave		
		Solvent	Free-solvent		Solvent	Free-solvent	
1	84	95	71	48	5	-	760
2	84	96	83	48	5	-	760
3	87	94	80	48	5	-	760
4	94	97	88	48	5	-	760

3.2Raman spectroscopy

For the assignment of the Raman signals, we considered the molecular structures with the corresponding atomic identification (**Fig. 2**). Both ligands and boron complexes can present tautomeric equilibrium between two isomers with the N1-C8 and C8-O2 bonds in amide or oxime groups. However, the crystallographic studies carried out on 1, 2 and 5, 6 suggest that the amide isomer is stabilized for the ligands through intermolecular and intramolecular hydrogen bonds. On the contrary, the complexes present the C8-O2 bond length closer to that of a single bond. Raman spectra were recorded by exciting at 785 nm, outside the absorption of the molecule in order to avoid any fluorescence effect.

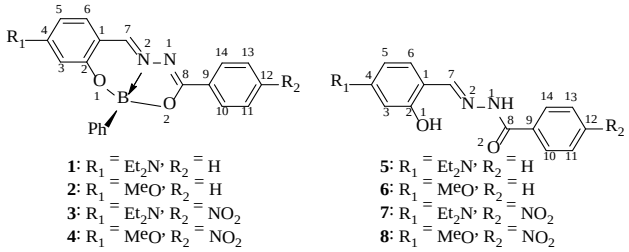

Fig. 2. Boron complexes 1-4 and their free-ligands 5-8.

The spectra of compounds **5**, **6,1** and **2** are showed as representative samples for the whole series (**Fig. 3**). The spectra are reported in the 1650-1500 cm^{-1} region, where changes in the chemical structures of the molecules due to the complexation can be associated with shifts in the corresponding double bonds vibrations. Table 2 collects the corresponding wavenumbers for all the molecules. The characteristic boron vibrations cannot be identified as they are expected at around

ISSN 2348 – 7968

1370 cm^{-1} for the asymmetric B-O stretching [24], between 1103 cm^{-1} and 1082 cm^{-1} for the ν B-C [25] and around 700 cm^{-1} for ν B-N [26]; falling in a region where many other vibrations (for instance C-O stretching, C-N bending) appear.

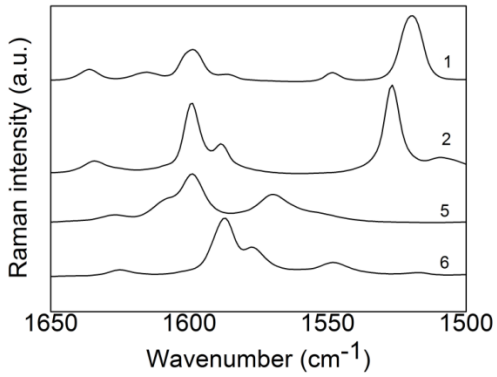

Fig. 3. Raman spectra of boron complexes **1**-**2** and free-ligands **5**-**8**.

For the free-ligands, considering the typical vibrations of the amide group, the middle band at 1625 cm^{-1} is the fingerprint of the amide I (C8-O2) vibration, while the strong signal in the 1550-1570 cm^{-1} region is of the amide II (NH stretching). Additionally to these bands, a strong signal at 1590-1600 cm^{-1} is observed and ascribed to the imine C=N (C7-N2) vibration. The complexation with boron converts the amide group to a rather an N=C-O- group with a vibration signal centered at c.a. 1635 cm^{-1} due to the C=N (N1-C8) vibration. The strong band at 1599 cm^{-1} was attributed to the -CH=CH- aromatic stretching vibration of the phenyl of the boronic group as reported by other authors [27]. The C=N stretching vibration of the imine group (N2-C7) that still appears as a strong vibration and is downshifted to around 1520 cm^{-1} because of the decrease in the bond strength as a consequence of the new dative bond. With the exception of the Ph vibration that is at the same wavenumber for the four complexes, as it is outside of the cyclic structure derived by the complexation, in general, the position of the bands for both ligands and complexes depends on the overall electronic contribution of the substituents in *para* position of the two termini phenyls as also observed in the optical properties.

Table 2: Selected Raman bands for boron compounds **1**-**4**, and free-ligands **5**-**8**.

Compound	Raman band (cm^{-1})	Assignment
1	1633, 1599, 1528	C=N (N1-C8), Ph. C=N (N2-C7)
2	1636, 1599, 1519	C=N (N1-C8), Ph. C=N (N2-C7)
3	1645, 1593, 1530	C=N (N1-C8), Ph. C=N (N2-C7)
4	1637, 1599, 1530	C=N (N1-C8), Ph. C=N (N2-C7)
5	1625, 1587	Amide I, amide II
6	1627, 1596	Amide I, amide II
7	1633, 1587	Amide I, amide II
8	1623, 1597	Amide I, amide II

3.3Optical linear and nonlinear properties

In order to investigate the photophysical properties, the UV-vis absorption and emission spectra of boron compounds **1**-**4** in toluene, chloroform and acetone were recorded. The experimental results are comparedwith calculated values by theoretical study in Table 3, and the UV-vis and emission spectra in different solutions are showed in Fig. 3andFig. 4. The UV-vis absorption spectra show a low energy broad band at 320 to 500 nm assigned to the π–π* transitions of the compounds. A change of solvent from toluene to chloroform and acetone revealed a blue/red shift around 23 to 70 nm for **2** and **3**. In the case of **1** and **4**, the main emission peak seems rather insensitive to the change to the solvents.

ISSN 2348 – 7968

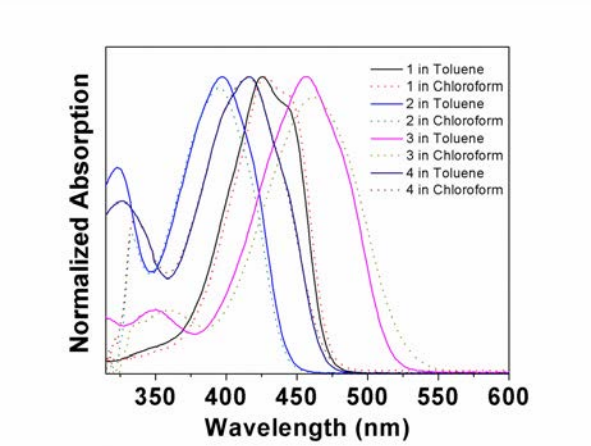

Fig. 4. Absorption spectra of boron compounds **1**-**4** in different solutions.

For the emission spectra in different polar solvents (Fig. 4), the molecule **3** displays a remarkable displacement from the red to blue region at room temperature while **2**showsa slight red shift.In the case of the emission band the compounds **3** and **4** do not emit in acetone solution. This suggests that the change of polarity solvent affects the geometry at the excited state.

Table 3: Calculated values of maximum absorption wavelength using TDDFT at the level B3LYP/6-311++G**//B3LYP/6-31G* and PCM solvent model (where applicable).

Compound	Solvent	λ_{max} (exp) [nm]	λ_{max} (calc) [nm]	Absorption Transition	λ_{emi} (exp) [nm]
1	None	n.d.	408	π-π*	n.d.
	Toluene	426	421	π-π*	489
	$CHCl_3$	428	422	π-π*	483
	Acetone	428	421	π-π*	483
2	None	n.d.	393	π-π*	n.d.
	Toluene	397	399	π-π*	470
	$CHCl_3$	395	396	π-π*	453
	Acetone	391	393	π-π*	469
3	None	n.d.	506	π-π*	n.d.
	Toluene	457	561	π-π*	528
	$CHCl_3$	461	586	π-π*	598
	Acetone	456	607	π-π*	n.l.
4	None	n.d.	452	π-π*	n.d.
	Toluene	417	477	π-π*	n.l
	$CHCl_3$	416	486	π-π*	518
	Acetone	409	493	π-π*	n.l.

n.d. = not determined, n.l. = not luminescent.

ISSN 2348 – 7968

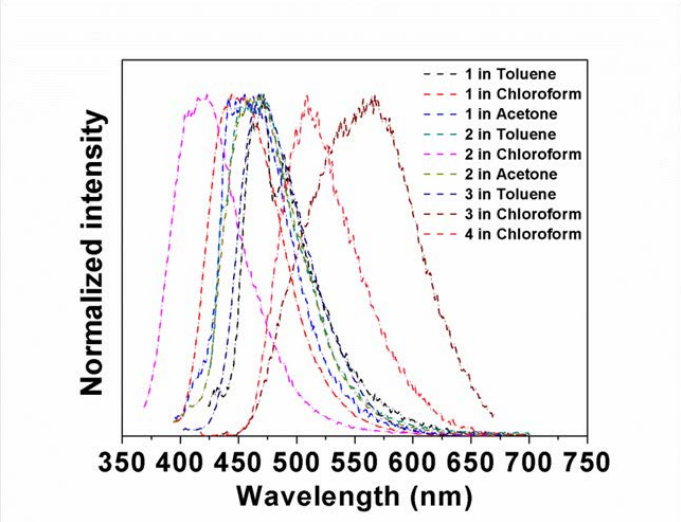

Fig.4. Emission spectra of boron compounds **1**-**4** in different solutions.

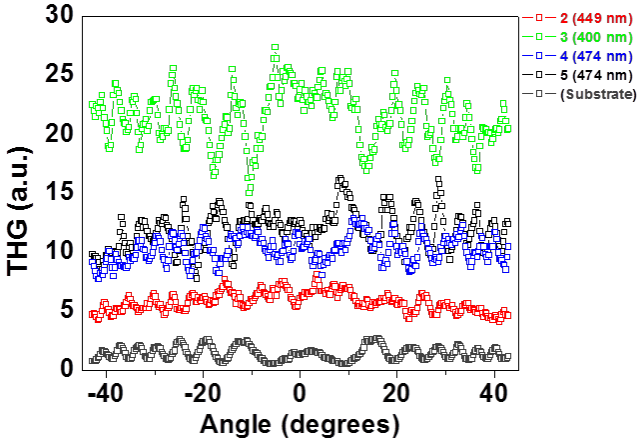

Fig. 5. THG Maker-fringe patterns for thin solids film doped with 30 wt% of compounds **2**-**4** and **5** for a 1-mm thick substrate without a film deposited on it. The fundamental wavelength is 1300 nm.

Typical plots of the THG signal from solid PS films doped with compounds **2**-**4** and from the substrate alone as functions of the incident angle for the excitation beam are showed (Fig. 5). The excitation wavelength in this case is 1300 nm with THG signal at 433 nm. The THG curves display an oscillatory behavior typical of Marker-Fringe pattern with average intensity values for the solid films between 4 to 15 times more intense than the substrate alone. The third order nonlinear susceptibilities for the free ligands and their complexes are summarized in Table 4. For ligands **6**-**8**, and the boron complex **2**,the THG signal was very weak and below the range of sensitivity for our experimental setup, so the estimation of their χ^3 values was not possible. In the case of **3** the poor of solubility does not permit the preparation of solid films for the analysis. The modest nonlinearities values were observed for the compounds **1** and **5** having the strong donor Et_2N resulting to be 3.53 x 10^{-12} and 1.51 x 10^{-12}esu, respectively. It important to notice that the value of susceptibility for **1** is larger than boron complexes due to the thickness of the film (460 nm) but the ability to generate the THG intensity shows that the best materials are the molecules with dipolar design type *push-pull*, actually, the best response corresponding to the molecule **3** (Fig. 5)**.**However**,** the nonlinear susceptibility value determined for **1** is larger than those reported for other tridentates, and bidentate Schiff bases with similar thicknesses[28]. In thecases of the boron compounds **1**, **3**-**4**, the enhancement of the nonlinear properties it is observed from the ligand to their corresponding complexes, except **2**,which does not have the ability for to generate the nonlinear response. A similar behavior was observed by other authors for different four-coordinate boronates[29]. Unfortunately, it was not possible obtaining the crystal structure for **3** and **4**, for to

ISSN 2348 – 7968

make a comparison and confirm the effect of the conformation on the nonlinear behavior between ligand-free and complexes but these materials due to was not possible to obtain good monocrystal that could be characterized by single X-ray diffraction. However, the analysis of crystal structure for **1** and **2** suggested that tetrahedral character of boron atom in **1** generated a high deformation of conjugated π-system compared with molecule **2**, which could be explains the nonlinear optical response. This result is consistent with nonlinear properties in boron compounds derived from salicylideniminophenols[30].

3.4Thermal analysis

Simultaneous analysis of thermal stability of boron compounds **1-4** and the Schiff bases **5-8** were determined by differential thermal analysis (DTA) and thermogravimetric analysis (TGA) in the temperature range 25 to 600 °C under a nitrogen atmosphere. The melting transition (T_m) and decomposition temperature (T_{d5}) are summarized in Table 4. The decomposition temperature curves for the Schiff bases **5-8**, which exhibited thermal stability in the range of 233-286 ^oC are given in Fig. 6. In the case of free ligands **7** and **8**, the DTA curves (Fig. S7-S8) show an endothermic peaks at 112 ^oC and 100 ^oC with a loss of mass of 4.2 and 5.4 %, respectively, which is attributed to the dehydration process. Additionally, the free ligands showed a remarkable endothermic peak from 184 to 224 ^oC range due to the melting process, this thermal behavior has been reported for another Schiff bases [31].

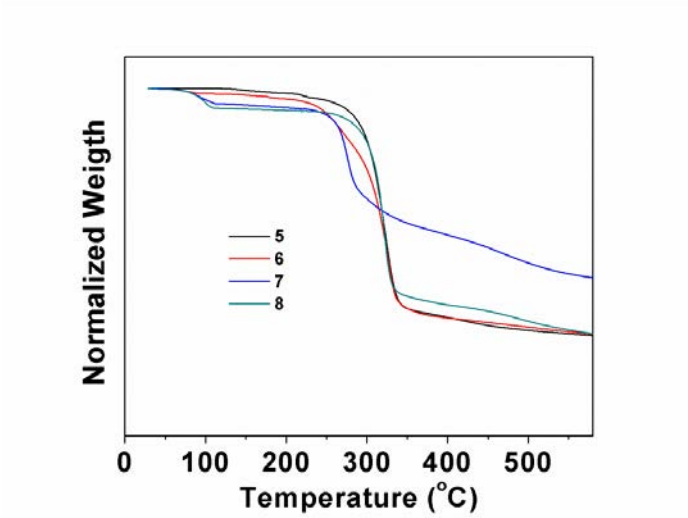

Fig. 6. TGA thermogram of Schiff bases **5-8**.

Table 4: Nonlinear properties into PS (30:70% wt.%) in solid state and thermal stability of boron complexes **1-4** and free-ligands **5-8**.

Compound	χ^3*10^{-12} [esu]	Td_5 [^oC]	Tm [^oC]
1	n. d.	278	217
2	1.51	225	216
3	3.39	230	151
4	2.42	243	172
5	3.53	286	224
6	n. d.	233	184
7	n. d.	261	224
8	n. d.	274	218

n. d. = not determined.

ISSN 2348 – 7968

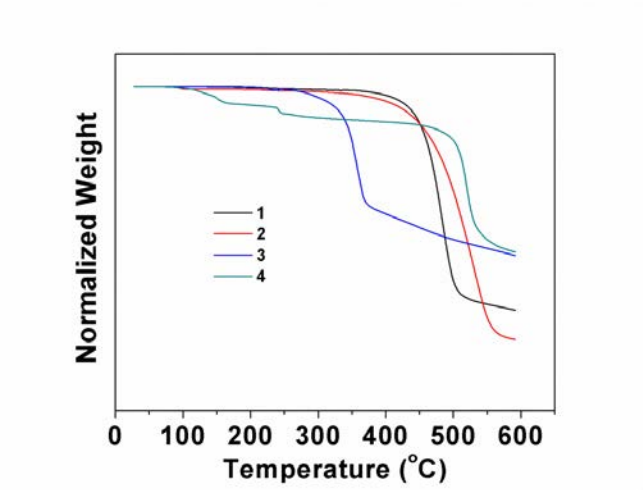

Fig. 7. TGA thermograms of boron compounds **1-4**.

3.5Electrochemical properties

The electrochemical parameters of all of the molecules are summarized in Table 5. It is important to point out that boron complexes undergo solvolysis during electrochemical studies in THF. Moreover, voltammograms are not resolved when are carried out in a complete cycle from -3 to +3 V window in CH_2Cl_2 or acetonitrile. In contrast, when they are analyzed individually, oxidation potentials are well defined in CH_2Cl_2, while reductions are in acetonitrile. The entire compounds show a first oxidation peak (reversible) between +0.8 and +1.6 V and a second but not well defined and irreversible peak at 1.7 - 2.0 V (Fig. S9), while in the reduction cycle two (quasi-reversible) peaks were observed for methoxy ligands and one (reversible) peak for their corresponding boron complexes (Fig. S10-S11).

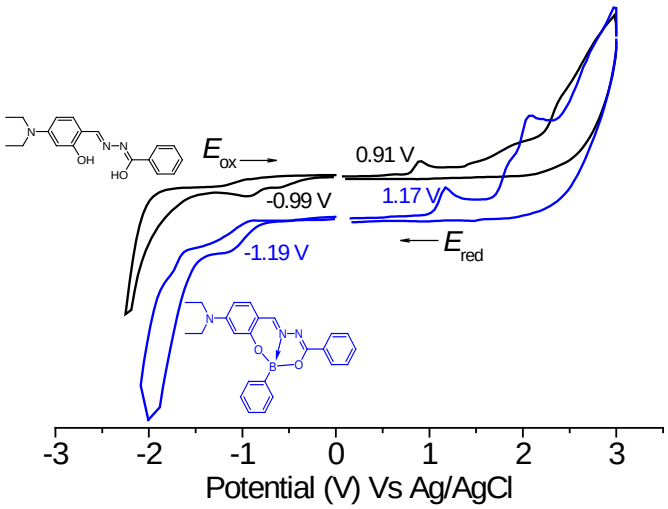

Fig. 8. Cyclic voltammograms of ligand **5** and its boron complex **1**.

ISSN 2348 – 7968

Table 5: Electrochemical properties of boron complexes and free-ligands.

Molecule	$^{a}E_{ox}^{max}$ [V]	$^{b}E_{red}^{max}$ [V]	*HOMO* [eV]	*LUMO* [eV]
1	+1.17	-1.19	-5.97	-3.61
2	+1.31	-1.21	-6.11	-3.59
3	+1.24	-1.06	-6.03	-3.74
4	+1.61	-1.10	-6.41	-3.70
5	+0.91	-0.94	-5.71	-3.86
6	+1.11	-0.91	-5.91	-3.89
7	+0.90	-0.95	-5.69	-3.85
8	+1.44	-1.07	-6.24	-3.73

[a]In CH_2Cl_2, [b] In acetonitrile.

In counterpart, the diethyl amino ligands exhibit two reduction peaks, which disappear to give rise just to one reversible peak before their complexation with Boron (Fig. 8). According to literature, the presence of more than one oxidative/reductive peak in the voltammograms of a conjugated molecule can be ascribed to the formation of polarons and bipolarons, but in these particular molecules we think that it is due to the separate contribution of the different functional groups of the molecules[32], such as is the case of these series of molecules bearing =N-N=, OH, Et_2N, NO_2, MeO and B groups. Therefore, for the present molecules, the first peak that appears in all the compounds in the oxidation potential, was associated with the loss of electrons of the N-N and/or C=O groups [33]. At this respect the oxidation potentials of complexes **1**-**4** become in general more positive than those of the corresponding free ligands **5**-**8**, for instances, the peak of complex **1** presents a shift of 0.256 V with respect to ligand **5**, 0.127 V for **2** and **6**, 0.34 V for **3** and **7** and of 0.174 V for **4** and **8**. This means that the boron quelated-ligands are more difficult to be oxidized than free ligands. Moreover, the higher values of oxidation potential are for those ligands and their complexes substituted with methoxy groups, and then by those molecules bearing the nitro group. Similar behavior was observed in the reduction cycle, where the potential reductions of boron complexes **1**-**4** are in general more negative than those of the corresponding free ligands, but less negative compared with the Alq3 (-2.1 V) that is the most widely used electron-transporting materials [34]. Therefore, their applications in light emitting diodes as electron-transporting compounds are a possibility.

3.6Theoretical calculations

The HOMO orbitals of all the compounds present the electronic distribution mainly on the Et_2N-or CH_3-O- group, up to the central amide for the ligands **5**-**8**, while for complexes **1**-**4**, the orbitals are extended up to the phenyl of the Boron; in other words all along the electron donor groups. In contrast, the LUMO orbitals are more localized on the electron acceptor groups of the molecules, which is in agreement with the push pull characters of the compounds. This effect being more marked for the nitro substituted complexes, which should present eventually larger nonlinear optical or photovoltaic properties. Fig. 9 shows the HOMO and LUMO orbital surfaces for ligand **4** and complex **8** as example, the orbitals for the other compounds are reported in the supporting information. Table 6 collects the calculated energy for the HOMOs and LUMOs. While the HOMO values are quite similar to the experimental ones obtained by cyclic voltammetry, the LUMO energies are less negative. However, calculations were realized based on an equilibrium conformer and in vacuum so the absolute values are not very significant. It is worth to observe that the phenyl of the boron is not involved in the electronic distribution in both HOMO and LUMO, as Boron is outside the conjugated plane. This can also explain why the Raman band at 1599 cm^{-1}, assigned to the aromatic C-C stretching of this phenyl does not shift along the complexes family.

ISSN 2348 – 7968

Molecule	HOMO	LUMO
8	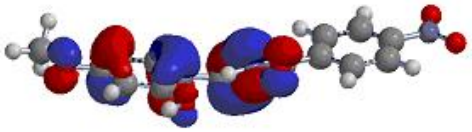	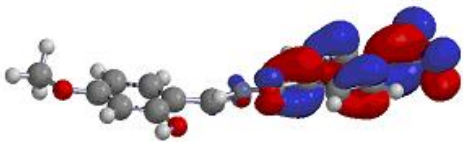
4	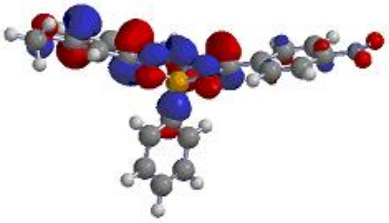	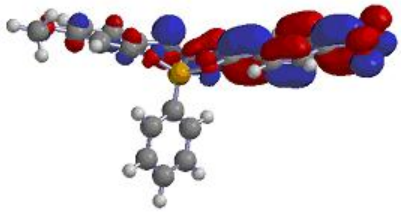

Fig.9 HOMO and LUMO orbital surfaces for ligand **8** and its corresponding complex **4**.

Table 6: Theoretical energy values for HOMO and LUMO orbitals of all the compounds.

Molecule	*HOMO* [eV]	*LUMO* [eV]
1	-5.2	-1.8
2	-5.6	-2.0
3	-5.5	-2.7
4	-6.0	-2.8
5	-5.2	-0.6
6	-5.9	-1.2
7	-5.4	-2.3
8	-6.0	-2.4

The figure 10 reports the electrostatic potential map (EPM) for the ligand **8** and its corresponding complex **4** with their optimized molecular geometry inserted for sake of discussion. The EPM of the other compounds is shown in the supporting information. The electrostatic potential maps for ligands shows a homogenous electron distribution map all along the ligands (green) (Fig. 10). From this figure, it can be observed that the lowest electrostatic potential density (blue) is mainly located on phenyls, -OH protons, while the carbonyl is the site surrounded by a great surface of negative charge, which represents the sites susceptible to redox potentials. Notice, that the nitro group in ligands **7**, **8** also shows a great surface of negative charge, while the –N-N- group exhibits a rather moderate electrostatic potential map. However, when ligands are boroncompound, the EPM images disclose that: i) for the complexes H terminated, a greatest surface of negative charge is centered in –O-B-O- and the out of the plane phenyl, ii) the presence of the nitro group allows a larger distribution of this negative electrostatic potential to the nitro, releasing the –O-B-O- in a moderate charge potential, iii) the lowest electrostatic potential surface is located in both the electron donor groups Et_2N- and Me-O-. On the basis of these results, we can assume that in the ligands the carbonyl, the nitro and in a slighter contribution the N-N- groups are the sites susceptible to redox potentials as was suggested by cyclic voltammetry, while in complexes the boron coordination groups and the nitro are the main sites.

ISSN 2348 – 7968

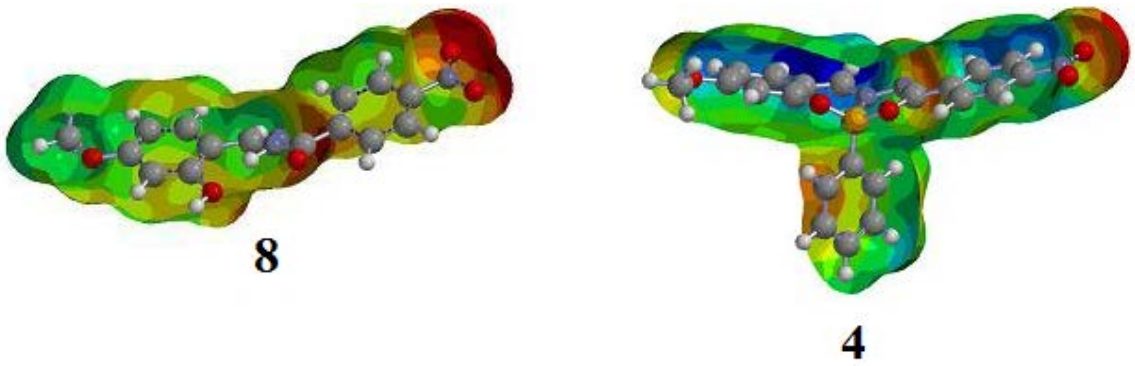

Fig.10. Electrostatic potential map for the ligand **8** and boron complex **4**.

4.Conclusions

In conclusion, we have developed an eco-friendly synthesis of boron compound derived from salycilidenbenzoylhydrazides. The boron compounds exhibit different absorption and emission behavior depending of the electronic contribution of the substituents in the*para* position of the two terminal phenyl rings. In general, the phenyl boron derivatives exhibit good thermal stability with a decomposition temperature range of 225-278 ^{o}C.The boron atom deviation from salicylidenimino-plane might affect the NLO response. By comparison with similar molecules in the literature,we found that the formation of the N→B coordinative bond increases the optical nonlinear response in comparison with the free-ligand. The electrochemical properties show that the boron complex are more difficult to be oxidized and reduced that the corresponding free ligands. Theoretical calculations of the boron compounds and their free-ligands indicated that phenyl of boron is not involved in the electronic distribution and that these orbital frontiers are extended along the electron donor (-NEt_2, -OMe) and acceptor (-NO_2) groups of each system.

Appendix A. Supplementary data

Supplementary data related to this article can be found at http://

Acknowledgements

Financial support from CONACYT (grant: 156450) and PAICYT-UANL (grant: CN886-11) is acknowledge as well as CONACYT scholarships for R. A. C. N. and M. C. G.

References:

[1] (a) Desiraju,G.R.Angew. Chem. Int. Ed. Engl. 34 (1995) pp 2311-2327; (b) Davis, C.J.; Lewis, P.T. Billodeux, D.R. Fronczek, F.R. Escobedo, J.O. Strongin, R.M. Org. Lett.3 (2001) pp 2443-2445.

[2]Killoran, J., Allen, L., Gallagher, J.F., Gallagher, W., M. O'Shea, D.F. Chem. Comm. 17 (2002) pp1862-1863.

[3](a) Kollmannsberger, M., Rurack, K. Resch-Genge, U. Daub, J. J. Phys. Chem. A. 102 (1998) pp10211-10220; (b) Kubo, Y., Yamamoto, M., Ikeda, M., Takeuchi, M., Shinkai, S., Yamaguchi, S., Tamao, K. Angew. Chem. Int. Ed. 42 (2003) pp2036-2040.

[4]Zeng, L., Miller, E.W., Pralle, A., Isacoff, E., Chang, C.J. J. Am. Chem. Soc. 128 (2006) pp10-11.

[5]Boyer, J.H., Haag, A.M., Sathyamoorthi, G., Soong, M.L., Thangaraj, K., Pavlopoulos, T.G. Heteroat. Chem. 4 (1993) pp39-49.

[6] (a) Wang, S. Coord. Chem. Rev. 215 (2001) pp79-98; (b) Huang, L.S. Chen, C.H. Mater. Sci. Eng. R. 39 (2002) pp143-222.

[7] Sun, Y., Rohde, D., Liu, Y., Wan, L., Wang, Y., Wu, W., Di, C., Yu, G., Zhu, D. J. Mater. Chem. 16 (2006) pp4499-4503.
[8] (a) Rao, Y.L., Amarne, H., Chen, L.C., Mosey, N., Wang, S. J. Am. Chem. Soc. 135 (2013) pp3407-3410; (b) Hudson, Z.M., Ko, S.B., Yamaguchi, S., Wang, S. Org. Lett. 14 (2012) pp5610-5613; (c) Rao, Y. Amarne, H. Wang, S. Org. Lett. 14 (2012) pp 5610-5613;
[9]Rodríguez, M., Ramos-Ortíz, G., Alcalá-Salas, M.I., Maldonado, J.L., López-Varela, K.A., López, Y., Domínguez, O.,Meneses-Nava, M.A., Barbosa-García, O., Santillán, R., Farfán, N. Dyes Pigm. 87 (2010) pp 76-83.
[10] (a) Höpfl, H., Farfan, N. J. Organomet. Chem. 547 (1997) pp71-77; (b) Höpfl, H., Sánchez, M. Barba, V., Farfán, N. Rojas, S., Santillán, R., Inorg. Chem. 37 (1998) pp1679-1692; (c) Farfán, N.,Höpfl, H.,Barba, V., Ochoa, M. E.,Santillán, R., Gómez, E., Gutiérrez, A.J. Organomet. Chem. 581 (1999) pp70-81;(d) Barba, V.,Cuahutle, D., Ochoa, M. E.,Santillán, R.,Farfán, N. Inorg. Chim.Acta. 303 (2000) pp7-11;(e) Abreu, A., Alas, S.J., Beltrán, H.I.,Santillán, R.,Farfán, N. J. Organomet. Chem. 691 (2006) pp 337-348; (f) Barba, V., Hernández, R.,Santillán, R.,Farfán, N. Inorg.Chim.Acta. 363 (2010) pp4112-4116;(g) Rivera, J. M., Méndez, E., Colorado-Peralta, R., Rincón, S., Farfán, N., Santillán. R. Inorg. Chim. Acta. 390 (2012) pp26-37.
[11] Reyes, H. Muñoz, B.M., Farfán, N., Santillán, R., Rojas-Lima, S.,Lacroix, P.G.,Nakatani, K. J. Mat. Chem. 12 (2002) pp2898-2903.
[12]Adib, M.,Sheikhi, E.,Bijanzadeh,, H.R. Zhu, L.G. Tetrahedron. 68 (2012) pp3377-3383.
[13] Muñoz, B.M., Santillán, R., Rodríguez, M., Méndez, J.M., Romero, M., Farfán, N.,Lacroix, P.G.,Nakatani, K., Ramos-Ortíz, G., Maldonado, J.L. J. Organomet. Chem. 293 (2008) pp 1321-1332.
[14] (a) Varma, R.S. Pure. Appl. Chem. 73 (2001) pp 193-198; (b) Varma, R.S. Tetrahedron 58 (2002) pp 1235-1255.
[15] (a) Zyss, J. Molecular nonlinear optics, materials Press Inc: USA, 1994; (b) Yuan, Z.,Entwistle, C.D.,Collings, J.C.,Albesa-Jové, D.,Batsanov, A.S., Howard, J.A.K. Chem Eur. J. 12 (2006) pp 2758-2771; (c) Entwistle, C.D.,Marder, T.B. Chem. Mater. 16 (2004) pp4574-4585;(d) Entwistle, C.D., Harder, T.B. Angew.Chem. Int. Ed. 41 (2002) pp2927-2931.
[16] (a) Reyes, H.,García, C.,Farfán, N.,Santillan, R.,Lacroix, P.G.,Lepetit, C.,Nakatani, K. J. Organomet. Chem. 689 (2004) pp 2303-2310; (b) Muñoz Blanca, M.,Santillán, R., Rodríguez, M., Méndez, J.M., Romero, M.,Farfán, N.,Lacroix, P.G.,Nakatani, K., Ramos-Ortíz, G., Maldonado, J.L. J. Organomet.Chem. 693 (2008) pp 1321-1434; (c) Rodríguez, M., Castro-Beltrán, R., Ramos-Ortíz, G., Maldonado, J.L., Farfán, N., Domínguez, O., Rodríguez, J., Santillán, R., Meneses-Nava, M.A., Barbosa-García, O. J. Synth. Met. 159 (2009) pp1281-1287;(d) Rodríguez, M., Maldonado, J.L., Ramos-Ortíz, G.,Lamére, J.F.,Lacroix, P.G., Farfán, N., Ochoa, M.E., Santillán, R., Meneses-Nava, M.A., Barbosa-García, O.,Nakatani, K. New J. Chem. 33 (2009) pp1693-1702.
[17] (a) Izumi, T.,Kobashi, S.,Takimiya, K., Aso, Y.,Otsubo, T. J. Am. Chem. Soc. 125 (2003) pp 5286-5287;
(b) Wang, H. Y Chen, G.Y., Liu, Hu, L.H., Xu, X.P., Ji, S.J. DyesPigm. 83 (2009) 269; (c) Mejer, H., Gerold, J., Kolshorn, H., Muhling, B. Chem. Eur. J. 10 (2004) 360-370; (d) Ning, Z.J., Zhang, Q., Pei, H.C., Luan, J.F., Lu, C.G., Cui, Y.P. J. Phys. Chem. 113 (2009) 10307-10313.
[18] Ramos-Ortiz, G., Maldonado, J.L., Meneses-Nava, M.A., Barbosa-García, O., Olmos, M. Opt. Mater. 29 (2007) pp636-641.
[19] Schmidt, M.W.,Baldridge, K.M.,Boatz, J.A.,Elbert, S.T., Gordon, M.S., Jensen, J.H.,Koseki S., Matsunaga, N. Nguyen, K.A., Su, S.,Windus, T.L.,Dupois, M.,MotgomeryJr, J.A. J. Comput. Chem. 14 (1993) pp 1347-1363.
[20] (a) Becke, A.J. Chem. Phys. 98 (1993) pp 56648; (b) Lee, C., Yang, W., Parr, R. Phys. Rev. B. 37 (1988) pp785-789; c) Vosko, S.H.,Wilk, L.,Nusair, M. Can. J. Phys. 58 (1980) pp1200;(d) Stephens, P., Devlin, F.,Chabalowski, C., Frisch, M. J. Phys. Chem. 98 (1994) pp11623-11627.
[21]Cossi, M.,Rega, N.,Scalmani, G.,Barone, V.J. J. Comput.Chem. 24 (2003) pp669-681.
[22]Allouche, A.R.J. J. Comput. Chem. 32 (2011) pp174-182.
[23] Chan-Navarro, R., Jiménez Pérez, V.M., Muñoz Flores, B.M.,Rasika Dias, H.V.,Moggio, I., Arias, E., Ramos-Ortíz, G.,Santillán, R.,García, C.,Ochoa, M.E,Yousufuddin, M.,Waskman, N. Dyes Pigm. 99 (2013) pp1036.
[24]Piergies, N.,Proniewicz, E., Ozaki, Y., Kim, Y.,Proniewicz, L.M. J. Phys. Chem. A. 117 (2013) pp5693-5707.
[25] (a) Faniran, J.A.,Shurvell, H.F. Can. J. Chem. 46 (1968) pp2089-2095; (b) Santucci, L., Gilman, H. J. Am. Chem. Soc. 80 (1958) pp193-196.
[26](a) Taylor, R.C.,Cluff, C.L. Nature 182 (1958) pp390-391; (b) Goubeau, J. Adv. Chem. Ser. 42 (1964) pp87-94; (c) Taylor, R.C. Adv. Chem. Ser. 42 (1964) pp 59.

ISSN 2348 – 7968

[27]Rodríguez, M.,Ramos-Ortíz, G., Alcalá-Salas, M.I., Maldonado, J.L., López Varela, K.A., López, Y., Domínguez, O., Meneses-Nava, M.A., Barbosa-García, O.,Santillan, R., Farfán, N. DyesPigm. 87 (2010) pp76-83.

[28]Rodríguez, M.,Maldonado, J.L., Ramos-Ortíz, G., Domínguez, O., Ochoa, Ma. E., Santillán, R., Farfán, N., Meneses-Nava, M.A.,Barbosa-García, O. Polyhedron 43 (2012) pp194-203.

[29]Rodríguez, M.,Castro-Beltrán, R.,Ramos-Ortíz, G.,Maldonado, J.L.,Farfán, N.,Domínguez, O.,Rodríguez, J.,Santillán, R.,Meneses-Nava, M.A.,Barbosa-García, O. J. Synthetic Met.159 (2009) pp1281-1287.

[30]Reyes, H.,Muñoz-Flores, B.M., Farfán, N.,Santillán, R.,Rojas-Lima, S.,Lacroix, P.G.,Nakatani, K. J. Mater. Chem. 12 (2002) pp2898-2903.

[31](a) Mohamed, G.G.,Omar, M.M.,Ibrahim, A.A. Eur. J. Med. Chem. 44 (2009) pp4801-4812; (b) Ceyhan, G.,Köse, M.,Tümer, M.,Demirtas, I.,Yağlioğlu, A.S.,McKee, V.J. Lumin. 143 (2013) pp623-634.

[32](a) Zotti, G.,Zecchin, S.,Schavon, G. Macromolecules 34 (2001) pp3889-3895;(b) Chandraselkhar, P. Conducting Polymers: Fundamentals and Applications, Kluwer Academic Publishers, USA, 1999; (c). Schenning, A.P.H.J.,Tsipsis, A.C.,Meskers, S.C.J.,Beljonne, D., Meijer, E.W.,Brédas, J.L. Chem. Mater. 14 (2002) pp1362-1368.

[33]Cakir, S.,Odabasoglu, M.,Bicer, E.,Yazar, Z. J. Mol. Struct. 918 (2009) pp81-87.

[34]Zhang, H.,Huo, C.,Ye, K.,Zhang, P.,Tian, W.,Wang, Y. Inorg.Chem. 45 (2006) pp2788-2794.